Measurement of the neutron capture cross section of ^{234}U in n_TOF at CERN

W. Dridi*[1], U. Abbondanno[2], G. Aerts[1], H. Álvarez[3], F. Alvarez-Velarde[4], S. Andriamonje[1], J. Andrzejewski[5], P. Assimakopoulos [6], L. Audouin [7], G. Badurek[8], P. Baumann[9], F. Bečvář[10], E. Berthoumieux[1], F. Calviño[11], D. Cano-Ott[4], R. Capote[12,31], A. Carrillo de Albornoz[13], P. Cennini[14], V. Chepel[15], E. Chiaveri[14], N. Colonna[16], G. Cortes[17], A. Couture[18], J. Cox[18], M. Dahlfors[14], S. David[7], I. Dillman[19], R. Dolfini[20], C. Domingo-Pardo[21], I. Duran[3], C. Eleftheriadis[22], M. Embid-Segura[4], L. Ferrant[7], A. Ferrari[14], R. Ferreira-Marques[15], H. Frais-Koelbl[12], K. Fujii[2], W. Furman[23], I. Goncalves[15], E. Gonzalez-Romero[4], A. Goverdovski[24], F. Gramegna[25], E. Griesmayer[12], C. Guerrero[4], F. Gunsing[1], B. Haas[26], R. Haight[27], M. Heil[19], A. Herrera-Martinez[14], M. Igashira[28], S. Isaev[7], E. Jericha[8], F. Käppeler[19], Y. Kadi[14], D. Karadimos[6], D. Karamanis[6], M. Kerveno[9], V. Ketlerov[14,24], P. Koehler[29], V. Konovalov[14,23], E. Kossionides[30], M. Krtička[10], C. Lampoudis[1,22], H. Leeb[8], A. Lindote[15], I. Lopes[15], M. Lozano[31], S. Lukic[9], J. Marganiec[5], L. Marques[13], S. Marrone[16], P. Mastinu[25], C. Massimi[32], A. Mengoni[12,14], P.M. Milazzo[2], C. Moreau[2], M. Mosconi[19], F. Neves[15], H. Oberhummer[8], S. O'Brien[18], M. Oshima[33], J. Pancin[1], C. Papachristodoulou[6], C. Papadopoulos[34], C. Paradela[3], N. Patronis[6], A. Pavlik[35], P. Pavlopoulos[36], L. Perrot[1], M.T. Pigni[8], R. Plag[19], A. Plompen[37], A. Plukis[1], A. Poch[17], C. Pretel[17], J. Quesada[31], T. Rauscher[38], R. Reifarth[27], M. Rosetti[38], C. Rubbia[20], G. Rudolf[9], P. Rullhusen[37], J. Salgado[13], L. Sarchiapone[14], I. Savvidis[22], C. Stephan[7], G. Tagliente[16], J.L. Tain[21], L. Tassan-Got[7], L. Tavora[13], R. Terlizzi[16], G. Vannini[32], P. Vaz[13], A. Ventura[39], D. Villamarin[4], M.C. Vincente[4], V. Vlachoudis[14], R. Vlastou[34], F. Voss[19], S. Walter[19], H. Wendler[14], M. Wiescher[18], K. Wisshak[19],

[1] *CEA/Saclay - DSM/DAPNIA, Gif-sur-Yvette, France*
[2] *Istituto Nazionale di Fisica Nucleare, Trieste, Italy*
[3] *Universidade de Santiago de Compostela, Spain*
[4] *Centro de Investigaciones Energeticas Medioambientales y Technologicas, Madrid, Spain*
[5] *University of Lodz, Lodz, Poland*
[6] *University of Ioannina, Greece*
[7] *Centre National de la Recherche Scientifique/IN2P3 - IPN, Orsay, France*
[8] *Atominstitut der Österreichischen Universitäten,Technische Universität Wien, Austria*
[9] *Centre National de la Recherche Scientifique/IN2P3 - IReS, Strasbourg, France*
[10] *Charles University, Prague, Czech Republic*
[11] *Universidad Politecnica de Madrid, Spain*
[12] *International Atomic Energy Agency (IAEA), Nuclear Data Section, Vienna, Austria*
[13] *Instituto Tecnológico e Nuclear(ITN), Lisbon, Portugal*
[14] *CERN, Geneva, Switzerland*
[15] *LIP - Coimbra & Departamento de Fisica da Universidade de Coimbra, Portugal*
[16] *Istituto Nazionale di Fisica Nucleare, Bari, Italy*
[17] *Universitat Politecnica de Catalunya, Barcelona, Spain*

*Corresponding author, Tel. +33-1-6908-2247, E-mail: Walid.Dridi@cea.fr

[18] University of Notre Dame, Notre Dame, USA
[19] Forschungszentrum Karlsruhe GmbH (FZK), Institut für Kernphysik, Germany
[20] Università degli Studi Pavia, Pavia, Italy
[21] Instituto de Física Corpuscular, CSIC-Universidad de Valencia, Spain
[22] Aristotle University of Thessaloniki, Greece
[23] Joint Institute for Nuclear Research, Frank Laboratory of Neutron Physics, Dubna, Russia
[24] Institute of Physics and Power Engineering, Kaluga region, Obninsk, Russia
[25] Istituto Nazionale di Fisica Nucleare(INFN), Laboratori Nazionali di Legnaro, Italy
[26] Centre National de la Recherche Scientifique/IN2P3 - CENBG, Bordeaux, France
[27] Los Alamos National Laboratory, New Mexico, USA
[28] Tokyo Institute of Technology, Tokyo, Japan
[29] Oak Ridge National Laboratory, Physics Division, Oak Ridge, USA
[30] NCSR, Athens, Greece
[31] Universidad de Sevilla, Spain
[32] Dipartimento di Fisica, Università di Bologna, and Sezione INFN di Bologna, Italy
[33] Japan Atomic Energy Research Institute, Tokai-mura, Japan
[34] National Technical University of Athens, Greece
[35] Institut für Isotopenforschung und Kernphysik, Universität Wien, Austria
[36] Pôle Universitaire Léonard de Vinci, Paris La Défense, France
[37] CEC-JRC-IRMM, Geel, Belgium
[38] Department of Physics and Astronomy - University of Basel, Basel, Switzerland
[39] ENEA, Bologna, Italy

Abstract

Accurate and reliable neutron capture cross sections are needed in many research areas, including stellar nucleosynthesis, advanced nuclear fuel cycles, waste transmutation, and other applied programs. In particular, the accurate knowledge of ^{234}U(n,γ) reaction cross section is required for the design and realization of nuclear power stations based on the thorium fuel cycle. We have measured the neutron capture cross section of ^{234}U at the recently constructed neutron time-of-flight facility n_TOF at CERN [2] in the energy range from 0.03 eV to 1 MeV with high accuracy due to a combination of features unique in the world: A high instantaneous neutron fluence and excellent energy resolution of the n_TOF facility, an innovative Data Acquisition System based on flash ADCs [3] and the use of a high performance 4π BaF_2 Total Absorption Calorimeter (TAC) as a detection device [4, 5].

In this paper, we will describe the experimental apparatus including the various TAC components and its performance. We also will present results from the ^{234}U(n,γ) measurement. A sample of 38.7 mg of $^{234}U_3O_8$ was pressed into a pellet and doubly encapsulated between Al and Ti foils which were 0.15 mm and 0.2 mm thick, respectively. Monte-Carlo simulations with GEANT4 [6] of the detector response have been performed. After the background subtraction and correction with dead time and pile-up, the capture yield from 0.03 eV up to 1.5 keV was derived. Preliminary analysis of the capture yield in terms of R-matrix resonance parameters is discussed.

KEYWORDS: Neutron capture cross section, neutron time of flight, Monte-Carlo simulations, 4π BaF_2 Total Absorption Calorimeter.

1. Introduction

Neutron capture cross sections are needed for many applications, in advanced nuclear fuel cycles and nuclear-waste transmutation, and are essential for the development and optimized design of these concepts. Many of the relevant isotopes have received less attention in the past, and at present the existing measured data are still insufficient, incomplete or sometimes even lacking. These isotopes with smaller relevance for the operation of present reactors will play an important role in the neutronics of future transmuters and in the assessment of their transmutation performance.

The neutron capture reaction cross section of ^{234}U, among others isotopes, needs to be measured since only two experimental data sets are available. The first one is a measurement by Muradyan *et al.* [7], the second one is a recent measurement performed at LANSCE [8].

For these reasons, in 2004 we have measured the neutron capture cross section of ^{234}U at the recently constructed neutron time-of-flight facility n_TOF at CERN [2] in the energy range from 0.03 eV to 1 MeV.

2. Experimental Setup

2.1 Features of the n_TOF facility

The neutron Time of Flight(n_TOF) facility at CERN is a neutron source with a wide energy range, where neurons are generated by spallation induced by 20-GeV/c protons onto a solid lead target. The proton beam has a time resolution of 6 ns (r.m.s.) and an intensity up to 7.10^{12} protons/pulse.

The lead spallation module has been designed in order to obtain the highest figure of merit (ratio between the neutron flux and a time resolution parameter squared). This results in a 80x80x60 cm^3 lead block with a 20-cm-deep niche in the entrance face. The target is water cooled. The water also acts as moderator for the outgoing neutron beam, strongly enhancing the neutron flux at low energies. At present the n_TOF neutron beam has two operational modes, one for capture and another for fission. This is achieved by interchanging the second collimator, located just in front of experimental area. This collimator has a diameter of 8.0 cm for fission measurements and 1.8 cm for capture.

2.2 ^{234}U sample

The sample of 38.7 mg of $^{234}U_3O_8$ (32.7 mg of ^{234}U, 0.231 MBq) was pressed into a pellet and doubly encapsulated between Al and Ti foils which were 0.15 mm and 0.2 mm thick, respectively, in order to fulfill the ISO 2919 certification requested by the safety regulations at CERN. It isotopic purity has been determinated by γ-ray spectroscopy and is $\geq 99\%$.

2.3 Data Acquisition System

The high instantaneous neutron flux at n_TOF, represents a great advantage especially for the measurements of small mass and radioactive samples as in our case, but it poses relevant problems on signal processing and acquisition due to pile-up events and large dead times. To overcome these problems, a Data Acquisition System (DAQ) based on fast digitizers has been used in the measurements consisting in 54 channels of high-performance Flash Analog to Digital Converter (FADC) with 8 bit resolution. Each channel has 16 Mbytes of memory and was operated at a sampling rate of 500 MSamples/s, thus allowing to detect the fast component

in the BaF_2 signals with sufficient resolution and recording of the full detector history for the entire neutron energy range. The raw data are sent to CERN's massive storage facility CASTOR via several Gbytes links. The amount of data produced during the measurements was about 2.5 Tbytes/day.

The n_TOF DAQ is running without acquisition dead time, and allows to perform a sophisticated signal analysis including pile-up discrimination, resulting in an excellent mechanism for controlling all kinds of systematic uncertainties associated with the detector's behavior.

2.4 Total Absorption Calorimeter

The design of the n_TOF Total Absorption Calorimeter (TAC) [10–14] is based on 40 BaF_2 crystals shaped as hexagonal and pentagonal truncated pyramids forming a spherical shell with 10 cm inner radius and 15 cm thickness. Each BaF_2 crystal is covered by a teflon light reflector layer and aluminum foil and a final cover with ^{10}B loaded carbon fiber capsule. The TAC has a high detection efficiency for for capture events near from 100% and an acceptable energy resolution (10% at 661.5 keV and 6% at 6.15% MeV). The targets are placed at the center of the TAC and surrounded by a neutron absorber made of $C_{12}H_{20}O_4(^6Li)_2$. The neutron absorber and the ^{10}B loaded carbon fiber capsule reduce the sensitivity of the detector to neutron scattering and do not reduce significantly the capture detection efficiency.

Energy calibration of each detector module are weekly performed by means of ^{137}Cs, ^{60}Co, ^{88}Y and Pu+C γ sources. In the interval the energy drift is monitored using the α intrinsic radioactivity of BaF_2 crystals.

Figure 1: Left: Picture of one hemisphere of the n_TOF TAC. The picture shows the neutron beam pipes, the central neutron absorber, and the ^{10}B loaded carbon fiber capsules. Right: Same view as implemented in the GEANT4 simulation.

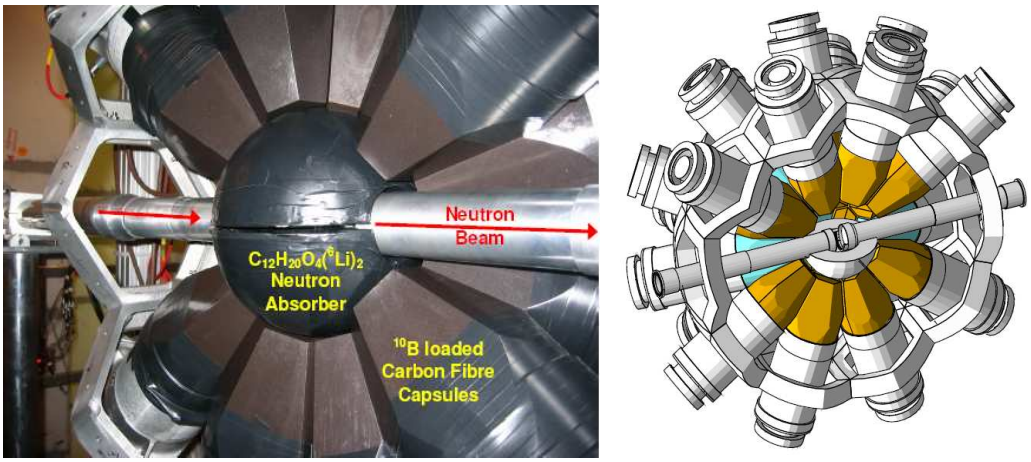

3. Data reduction procedure

The experimental yield, $Y(E)$, is determined using the following formula:

$$Y(E) = N \frac{S(E) - B(E)}{\nu(E)\, \varepsilon_{TAC}(E)} \quad (1)$$

where

- $S(E)$ is the number of neutrons of incoming energy E captured by the ^{234}U sample seen by the TAC
- $B(E)$ is the background at the neutron incoming energy E
- $\nu(E)$ is the number of neutrons of incoming energy E incident on the ^{234}U sample
- $\varepsilon_{TAC}(E)$ is the (energy dependent) TAC efficiency to detect neutrons captured by the ^{234}U sample
- N is a normalization coefficient (N $\approx$ 1)

3.1 Event selection criteria

In order to improve the signal to background ratio, one first needs to determine an optimal event selection criteria for the TAC. In our case, the main sources of background are :

- The sample radioactivity.
- Scattered neutrons captured by the TAC studied by means of a carbon sample.
- Scattered in beam gammas interacting with the TAC studied by means of a lead sample.

Although the sample is surrounded by a neutron absorber, and crystal capsules are doped with ^{10}B, above a few hundred eV the background is mainly due to scattered neutrons. This is because our samples were encapsulated in between two titanium foils as described before, in order to be ISO-2919 compliant. In order to minimize this component we keep only events for which more than one cluster is present and where a cluster consists of a connection of neighboring crystals that have been hit.

3.2 Background subtraction

The next step consists in determining the TAC energy response to a neutron captured by a ^{234}U nucleus with the previously defined event selection criteria. This is realized by studying the TAC response for a few resonances, as shown in figure 2 for the first resonance. To extract the signal from background, three histograms are needed:

1. The TAC response with the ^{234}U sample inside but without beam (radioactive background).
2. A bidimensionnal plot giving the TAC energy response at each time-of-flight bin with an empty canning sample (“scattering component” background).
3. A bidimensionnal plot giving the TAC energy response at each time of flight bin with the ^{234}U sample.

Then at each time-of-flight bin, the TAC response given by the last histogram, is decomposed in 3 components by performing a linear fit using the first two histograms (at the same time-of-flight for the “scattering component”) and the previously obtained TAC response to ^{234}U only.

Figure 2: TAC energy response for the first resonance of ^{234}U(n,γ) without any condition (in red) or requesting more than one cluster (in black)

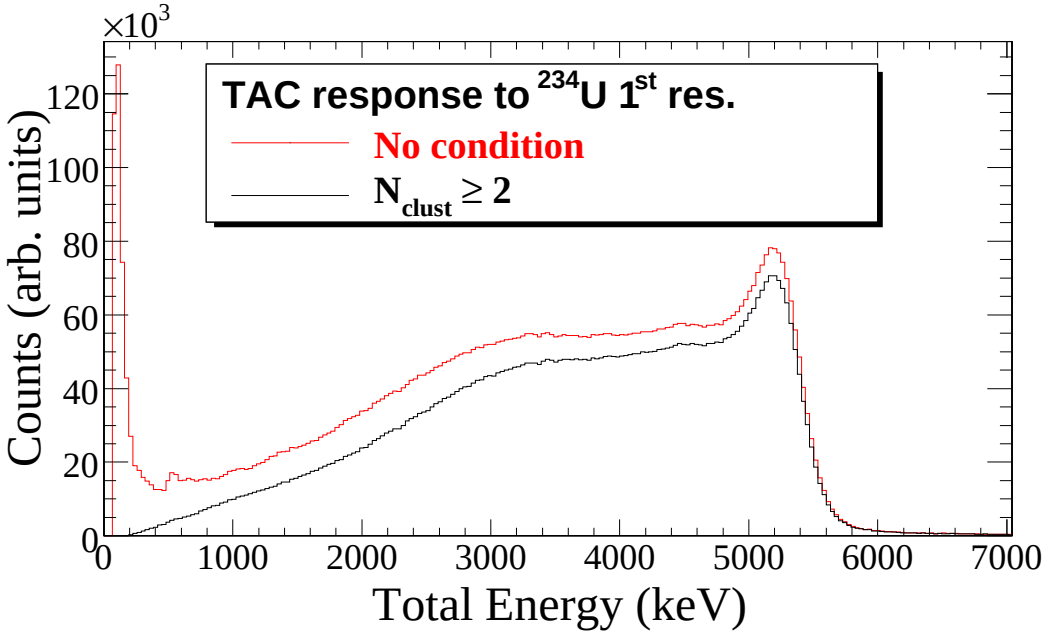

3.3 Efficiency determination

Although the data acquisition system used for this experiment works without introducing any dead time, the pulse shape algorithm used may fail to find a signal in the tail of another one. Because the counting rate can be very high, up to tens of MHz for the whole TAC, this efficiency loss has to be properly taken into account. To take care of this count rate dependence the efficiency term $\varepsilon_{TAC}(E)$ can be written:

$$\varepsilon_{TAC}(E) = \frac{\varepsilon_0 \, \varepsilon_{criteria}}{DT(E)} \tag{2}$$

where

- $\varepsilon_{criteria}$ is the efficiency of the event selection criteria, *i.e.* the probability to have more than one cluster hit.
- ε_0 is the TAC overall efficiency, *i.e.* the probability to detect at least one γ of the cascade.
- $DT(E)$ is the dead time correction factor.

In order to estimate the TAC overall efficiency and its count rate dependence a simulation has been performed. This consists in a γ-ray cascade generator from Bečvář [15] coupled to the GEANT4 [6] simulation toolkit. A dead time model has been included in the tracking package. This model is adjusted to reproduce the experimental histogram of interval time between two consecutive events in a given detector of the array. The dead time correction factor is then obtained by comparing the simulated TAC efficiency with the given criteria (more than one cluster) at various count rates to the one obtained without dead time effect.

Simulation also shows that the TAC overall efficiency, ε_0, is about 99% when no dead time effect is considered.

Figure 2 shows the TAC energy response to the first resonance of ^{234}U(n,γ) when all events are considered (in red), and for events where more than one cluster are involved (in black). The criteria efficiency, $\varepsilon_{criteria}$, is given by the ratio of the number of counts of the two histogram corrected by the dead time factor associated with the resonance. The deduced efficiency is 78$\pm$1%.

3.4 Time of flight to energy relation

The distance from the ^{234}U sample to the target moderator is 184.9$\pm$0.1 m. We took the "n_TOF default" resolution function as defined in SAMMY 1.0.8 [16].

3.5 Flux determination

For the flux above 0.7 eV, in the present analysis we took the n_TOF standard flux multiplied by the fraction of beam seen by the sample. This latter quantity is computed by simulation and the value found is 19.8%.

From 0.03 to 0.7 eV the flux seen by sample has been deduced from a gold capture measurement performed in similar conditions as the ^{234}U measurement.

3.6 Normalization

Finally the yield has been normalized in order to reproduce the ENDF/B-VI.8 [19] ^{234}U(n,γ) cross section in the thermal region *i.e.* below 0.1 eV.

4. Preliminary results and discussion

4.1 Yield in the thermal energy region

Table 1: Comparison between ENDF/B-VI.8 resonance parameters and our results at low energy ($E_n \leq$10 eV).

ENDF/B-VI.8			Our results		
E_n (eV)	Γ_γ (meV)	Γ_n (meV)	E_n (eV)	Γ_γ (meV)	Γ_n (meV)
-2	40	3.22	-0.97$\pm$0.01	26$\pm$2	0.85$\pm$0.06
5.16	40	3.92	5.1570$\pm$0.0003	39.0$\pm$0.1	3.62$\pm$0.01

Figure 3 shows the neutron capture yield on ^{234}U from 0.03 to 10 eV. Black symbols are our data. The red curve corresponds to a SAMMY simulation using ENDF/B-VI.8 resonances parameters. And finally the blue curve gives the SAMMY fit on our data. Although our data are normalized to reproduce the known cross section in a thermal spectra, one can clearly see on figure 3 that the slope given the ENDF/B-VI.8 yield does not correspond to the one given by our data. Table 1 shows a SAMMY fit on our data, compared to the ENDF/B-VI.8 adopted values. The quoted errors are only statistical. One should add a 0.1% error for the resonance energies due to the uncertainty in the flight path length. For the negative energy we found a radiation width of 26 meV, in agreement with Mughabghab value [17], which also correspond to the JENDL-3.3 [20] evaluation, and is smaller than the ENDF/B-VI.8 value. Nevertheless one should note our negative energy and neutron width does not correspond to the value of Mughabghab or JENDL. But since no differential measurement has been reported up to now down to thermal energy for this reaction, the radiation width for the negative energy was taken

Figure 3: Neutron capture on ^{234}U yield in the thermal region and for the first resonance obtained in the present experiment.

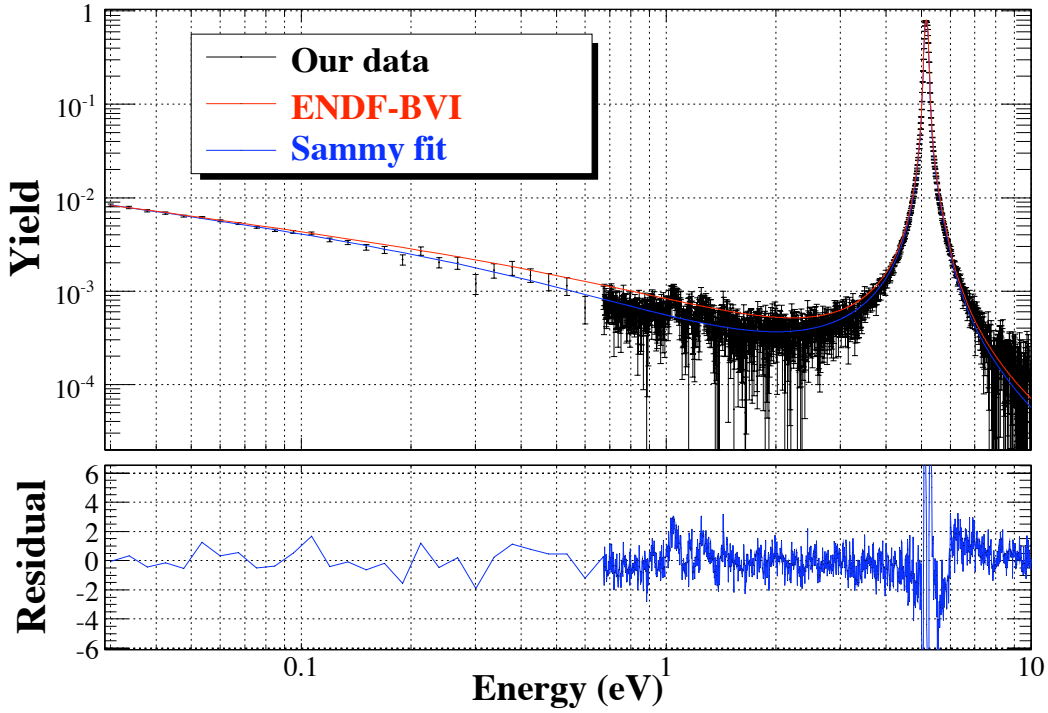

equal to that of the first resonance, and the other parameters being adjusted to reproduce the maxwellian averaged thermal cross section.

On the contrary the radiation width for the first ^{234}U(n,γ) resonance is close to the ENDF/B-VI.8 value, but with a variance comparable to that of JENDL-3.3 or Mughabghab. Our neutron width is about 8% lower than that of ENDF/B-VI.8. Nevertheless, as can be seen on figure 3, our best fit is not able to fairly reproduce the shape of the first resonance. Several reasons can be invoked to explain such a discrepancy. Firstly the free gas model, chosen in the present analysis to take care of Doppler broadening, is probably not well suited to describe this phenomenon for an oxide target. Secondly our sample description included in the SAMMY fit is inaccurate. In reality our sample consists of different layers of Ti-Al-U_3O_8. In SAMMY it is treated as an homogenous mixture of all these components. The impact of such a difference in the multiple scattering effect has not yet been investigated. And at last, some systematics may still remain in the data reduction procedure. The ongoing work consists in the comparison of the experimental yield using several independent procedures.

4.2 Average radiation width

The main discrepancy between the various evaluations is the average radiation width. ENDF/B-VI.8 gives a value of 40 meV based on the transmission measurement from James *et al.* [18] On the contrary the evaluation of JENDL-3.3 follows Mughabghab and gives 26 meV.

In order to disentangle these two values we performed a SAMMY analysis leaving free the radiation width of most of the resonances up to 200 eV. Above this energy our statistics is too low to allow to fit this parameter. The results are shown in figure 4. The resonance at 23 eV is not seen in the present data, but the parameters for the 22 eV resonance are close to

Figure 4: Comparison between experimental (black), ENDF/B-VI.8 (red), and SAMMY fit (blue) of neutron capture yield on ^{234}U up to 200 eV.

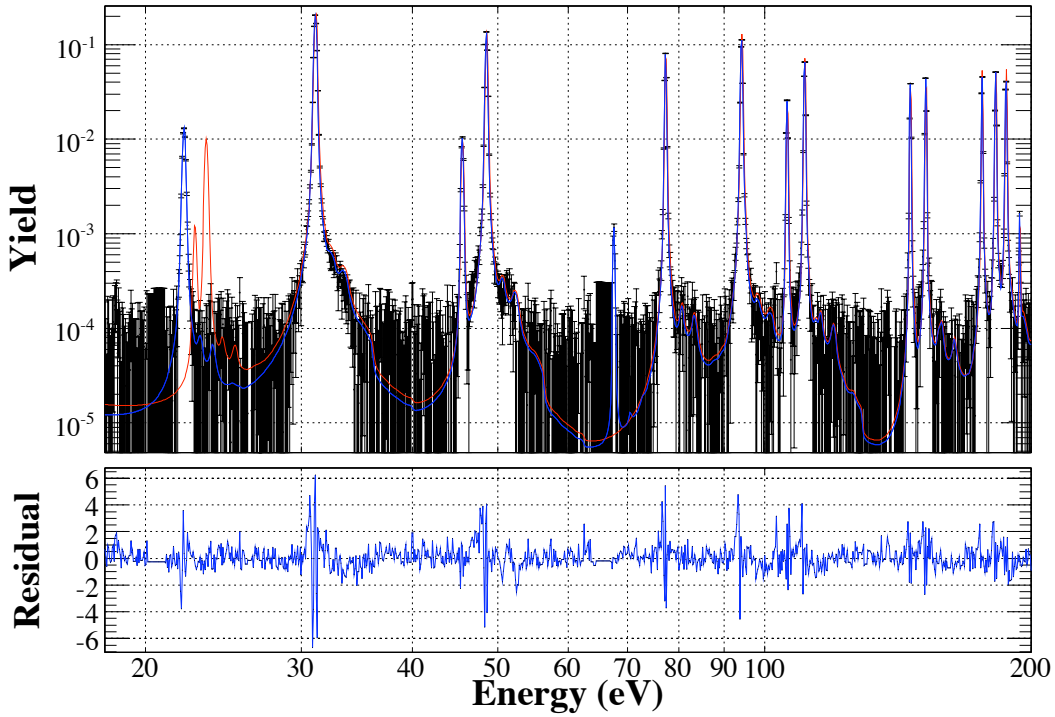

the ENDF/B-VI.8 23 eV resonance instead of the 22 eV one. We see a resonance at 67.6 eV that is not reported in others evaluations. For the others resonances, one can see a reasonable agreement between our SAMMY fit and the ENDF/B-VI.8 evaluation.

The preliminary average radiation width found in the present analysis is $\langle \Gamma_\gamma \rangle = 36 \pm 1.5$ meV.

5. Conclusion

A measurement of the neutron capture cross section of ^{234}U has been performed at the n_TOF facility at CERN, using the newly constructed 4π BaF_2 Total Absorption Calorimeter. A yield from 0.03 eV to 1.5 keV has been extracted, that allows to give some preliminary results. New parameters have been extracted to describe the cross section in the thermal energy domain. The first resonance radiation width found is 39 meV in accordance with ENDF/B-VI.8 value. The average radiation width for resonances below 200 eV is around 36 meV.

Acknowledgements

We acknowledge the CERN participation in the n_TOF project. This work has been supported by the European Commission's 5th Framework Programme under contract FIKW-CT-2000-00107.

References

1) Accelerator Driven Systems and Fast Reactors in Advanced Nuclear Fuel Cycles, ISBN 92-64-18482-1 ENEA/OECD Report, 2002.

2) U. Abbondano *et al.*, "n_TOF Performance Report", CERN/INTCO-011, INTC-2002-037.

3) R. Plag *et al.*, Nucl. Instr. and Meth. A **538** (2005) 692.

4) M. Heil *et al.*, Nucl. Instr. and Meth. A **459** (2001) 229.

5) D. Cano-Ott *et al.*, Proceeding of Int. Conf. Nucl. Data for Sci. and Tech. (ND2004) Santa Fe, New Mexico (USA), 26 September - 1 October 2004, p.1442.

6) S.Agostinelli *et al.*, Nucl. Instr. and Meth. A **506** (2003) 250.

7) G.V. Muradyan *et al.*, *Measurements of Neutron Capture Cross Sections of* ^{234}U *and* ^{236}U *and Fission Cross Section of* ^{236}U, Proceeding of 7^{th} International Seminar on Interaction of Neutrons with Nuclei (ISINN-7). Dubna, May 25-28,1999, **JINR E3-98-212** p.292

8) J.L. Ullmann *et al.*, *The detector for advanced neutron capture experiments: A* 4π BaF_2 *detector for neutron capture measurements at LANSCE*, Proceeding of Int. Conf. Data for Sci. and Tech.(ND2004) Santa Fe, New Mexico (USA), 26 September - 1 October 2004, p.918.

9) E. Berthoumieux, *Preliminary report on* BaF_2 *Total Absorption Calorimeter test measurement*, CEA-Saclay/DAPNIA/SPhN, France (2004).

10) K. Wisshak *et al.*, *Large Barium Fluoride Detectors*, Nucl. Instr. and Meth. A **227** (1984) 91.

11) K. Wisshak *et al.*, *Prototype Crystals for the Karlsruhe* 4π *Barium Fluoride detector*, Nucl. Instr. and Meth. A **251** (1986) 101.

12) K. Wisshak *et al.*, *The Karlsruhe* 4π *Barium Fluoride detector*, Nucl. Instr. and Meth. A **299** (1990) 60.

13) K. Wisshak *et al.*, *Gamma-ray spectroscopy with a cooled Barium Fluoride crystal*, Nucl. Instr. and Meth. A **259** (1987) 583.

14) M. Heil *et al*, *A* 4π BaF_2 *detector for (n,*γ*) cross-section measurements at a spallation neutron source*, Nucl. Inst. and Meth. A **459** (2001) 229.

15) F. Bečvář, *Simulation of* γ *cascade in complex nuclei with emphasis on assessment of uncertainties of cascade-related quantities*, Nucl. Inst. and Meth. A **417** (1998) 434.

16) N.M. Larson, *Updated user's guide for SAMMY: Multilevel R-Matrix fits to neutron data using Bayes equations.*, **ORNL/TM-9179/R7**, Oak Ridge National Laboratory, 2006.

17) S.F. Mughabghab, *Atlas of Neutron Resonances,* 5^{th} *edition*, Elsevier ed., 2006.

18) G.D. James *et al.*, *Intermediate structure studies of* ^{234}U *cross sections*, Phys. Rev. **C 15**, (1977) 2083.

19) National Nuclear Data Center homepage, http://www.nndc.bnl.gov/.

20) Nuclear Data Center, Japan Atomic Energy Agency, http://wwwndc.tokai-sc.jaea.go.jp/jendl/jendl.html